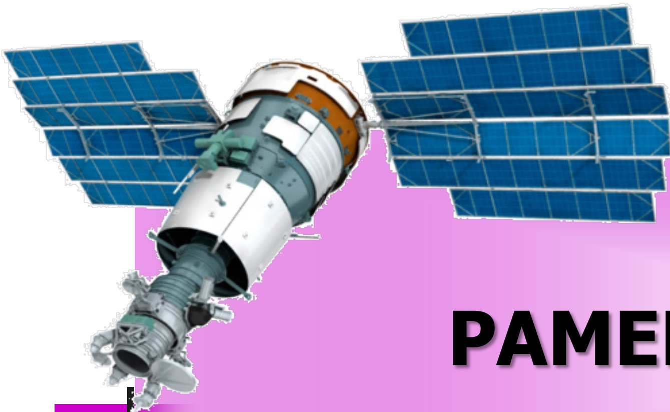

PAMELA Data Exploitation

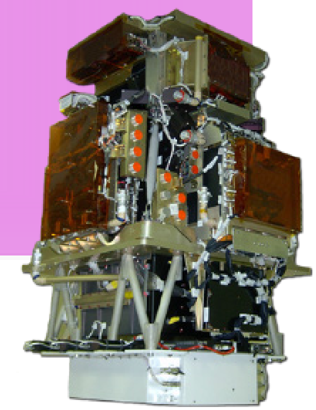

A. Bruno & F. Cafagna
INFN, Sezione di Bari, Italy

INFN Istituto Nazionale di Fisica Nucleare

PaMeLa a Payload for Antimatter Matter Exploration and Light-nuclei Astrophysics

esa

ESA & CNES Final Presentations :
Space Environments and Radiation Effects on EEE components
6 March 2017

Background and objectives

- Despite the significant improvements made in the last decades, the modeling of the near-Earth proton radiation environment is still incomplete, with largest uncertainties affecting the description of the high-energy (>50-100 MeV) fluxes in the inner zone and the South Atlantic Anomaly (SAA).

- ✓ These are exactly the observational objectives that can be addressed by the **PAMELA** experiment at LEO

- ➢ This work is aimed to provide a comprehensive characterization (energy spectra, angular & spatial distributions, etc.) of the high-energy (>70 MeV) geomagnetically trapped proton fluxes in the SAA, and a preliminary comparison with the current empirical models

The PAMELA collaboration

Payload for Antimatter Matter Exploration and Light-nuclei Astrophysics

Italy: Bari, Florence, Frascati, Naples, Rome, Trieste, CNR, Florence

Russia: Moscow, St. Petersburg

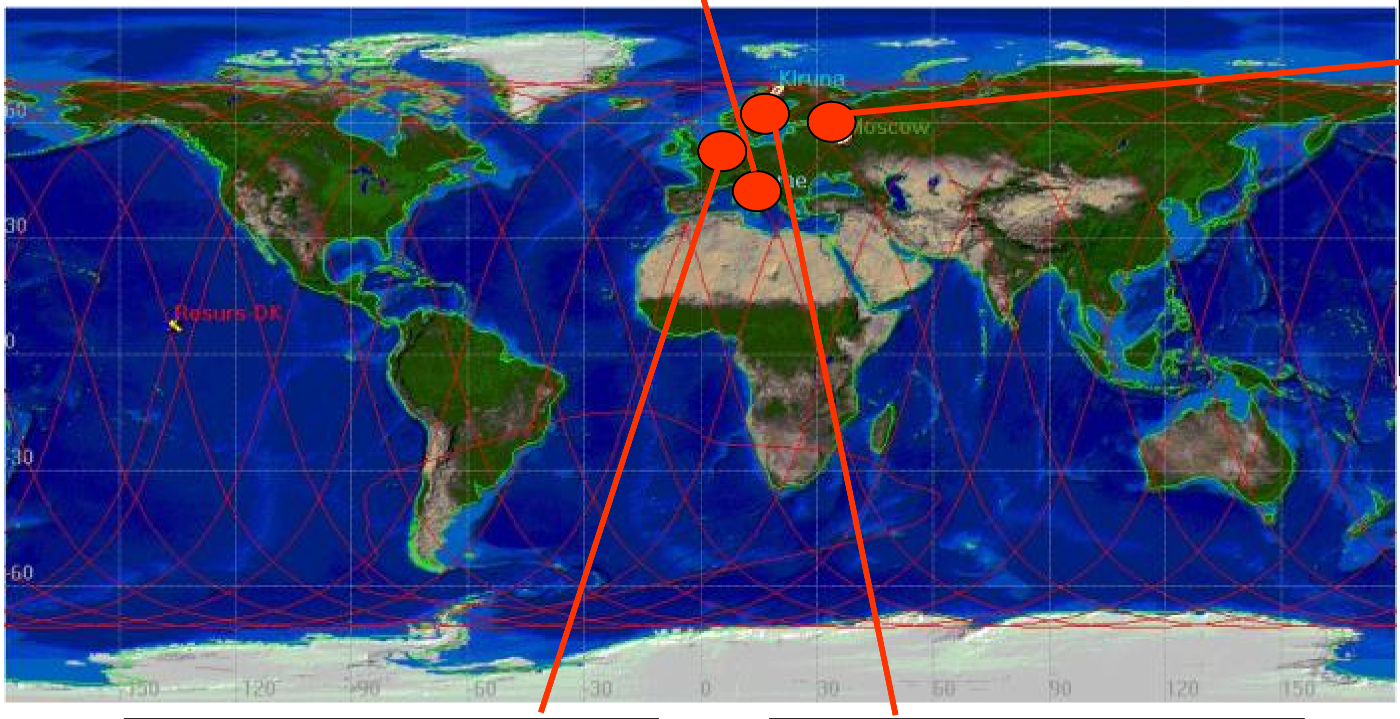

Germany: Siegen

Sweden: KTH, Stockholm

The PAMELA experiment

Main requirements → high-sensitivity particle identification and precise momentum measure

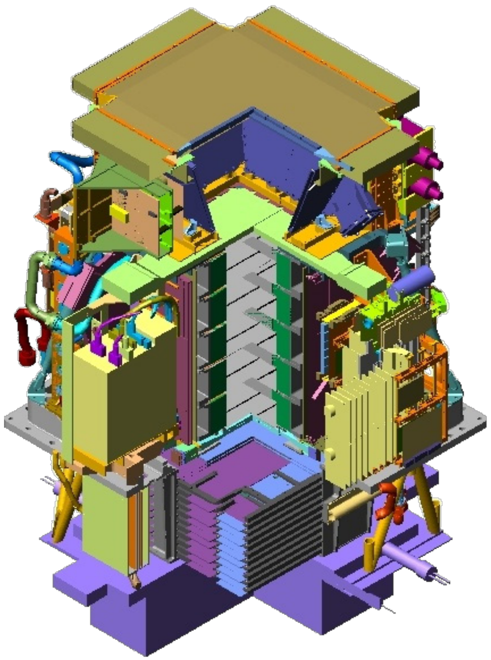

Size: 130x70x70 cm^3
GF: 21.5 cm^2 sr
Mass: 470 kg
Power Budget: 360W

Resurs DK-1 satellite:
Semi-polar (70° inclination) and elliptical (350÷610 km altitude) orbit

Time-Of-Flight
plastic scintillators + PMT
- Trigger
- Albedo rejection;
- Mass identification up to 1 GeV;
- Charge identification from dE/dX.

Anticoincidence shield
plastic scintillators + PMT

Electromagnetic calorimeter
W/Si sampling (16.3 X_0, 0.6 λI)
- Discrimination e+ / p, anti-p / e^- (shower topology)
- Direct E measurement for e^-

Bottom scintillator (+PMT)

Neutron detector
^{3}He counters
- High-energy e/h discrimination

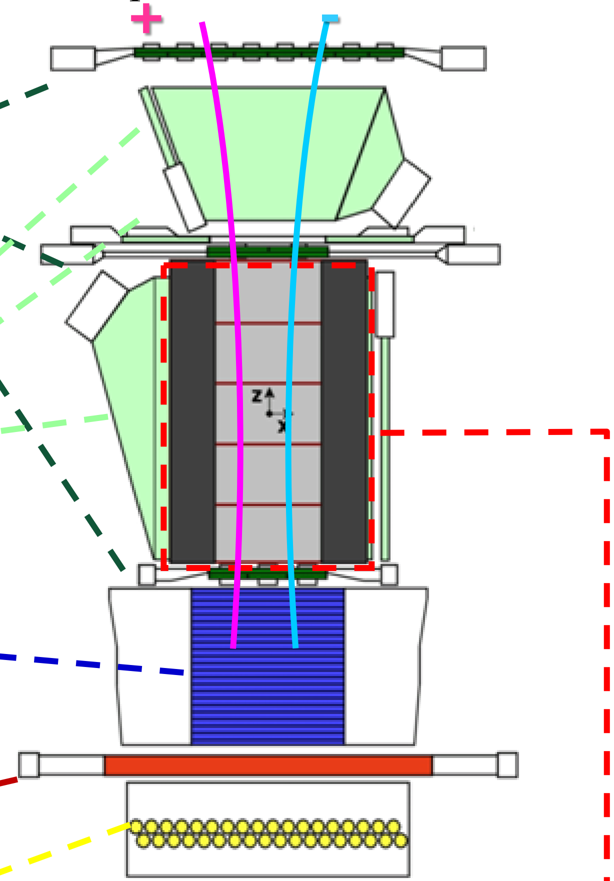

Spectrometer
microstrip silicon tracking system + permanent magnet
- Magnetic rigidity: R=pc/Ze
- Charge sign
- Charge value from dE/dx
- Particle direction

PAMELA scientific goals


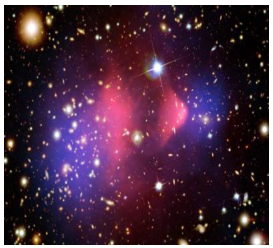
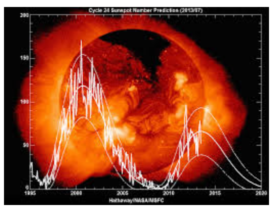
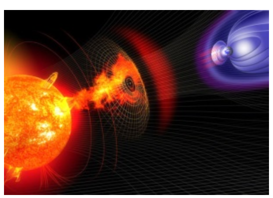
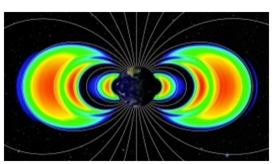

Precise measurements of protons, electrons, their antiparticles and light nuclei in the cosmic radiation

- Research for Dark Matter indirect signatures
- Exploration of the particle/antiparticle symmetry
- Investigation of the cosmic-ray origin and propagation mechanisms in the Galaxy, the heliosphere and the terrestrial magnetosphere
  - detailed measurement of the high energy particle populations (galactic, solar, geo-magnetically trapped and albedo) in the near-Earth radiation environment

PAMELA measurements at LEO

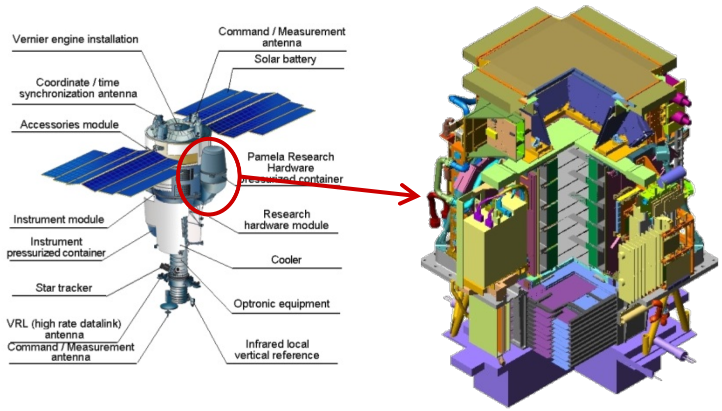

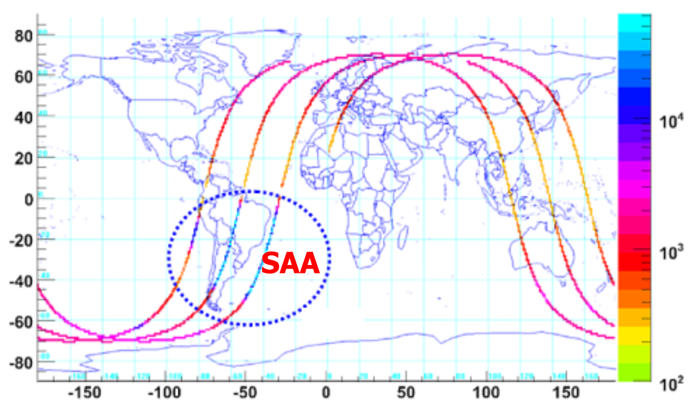

- Semi-polar (70 deg) and elliptic (350 - 610 km) orbit
  - polar caps (low energy CRs & SEPs)
  - geomagnetically trapped (SAA) and albedo (all latitudes)
- Precise rigidity measurements
  - wide range (≥400 MV)
- Good angular resolution (~2 deg)
  - possibility to investigate flux anisotropies
- Sensitive to particle composition
  - p/pbar, e+/e-, light nuclei

This work is based on the proton data acquired by PAMELA between July 2006 and September 2009

The particle classification algorithm

PAMELA data:
- **spacecraft position & orientation**
- **particle rigidity and direction**

(provided by the tracking system)

IMF, SW and geomagnetic parameters:
- **high-resolution (5-min) OMNIWeb data**

NASA/Goddard Space Flight Center

NB: the magnetospheric configuration is **updated event by event**, intepolating involved parameters

TRAJECTORY TRACING CODE

Runge-Kutta integration of motion equations
- **Based on Smart & Shea (2000, 2005)**

Realistic description of the geomagnetic field:
- internal sources: **IGRF11**
- external sources: **TS05/TS07D**

Trajectories propagated back and forth from the measurement location with no limit on tracing time/path

Interplanetary (SCR+GCR)
- **(back-traced) trajectories escape the model magnetosphere**

Albedo
- **(back-traced) trajectories intersect the atmosphere (40km)**

Geomagnetically trapped
- **trajectories perform more than ~$10^6/R^2$ steps for both propagation directions (≥4 drift cycles)**

NB: step-length ~1% of particle gyro-distance in the magnetic field

Data analyzed in the frame of **adiabatic theory** of particle motion in the geomagnetic field

Gyro motion:

- V x B acceleration leads to gyro motion about field lines
- frequencies ~kHz
- associated 1st invariant μ, relativistic magnetic moment:

$$\mu = \frac{p^2 \sin^2 \alpha}{2 m_0 B}$$

pitch angle α: $\tan\alpha = \frac{V_\perp}{V_\parallel}$

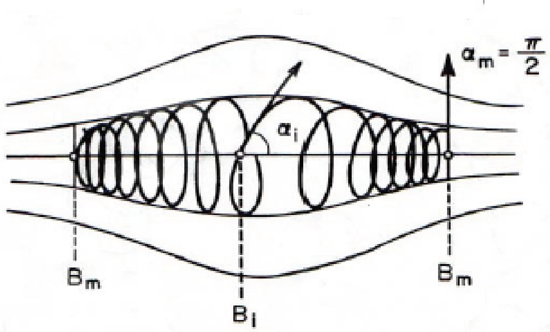

Bounce motion:

- As a particle gyrates down field line, the pitch angle increases as B increases
- Motion along field line reverses when pitch angle reaches 90° (mirror point)
- period ~sec
- associated 2nd invariant K longitudinal invariant:

$$K = \int_{-l_m}^{+l_m} p_\parallel \, dl$$

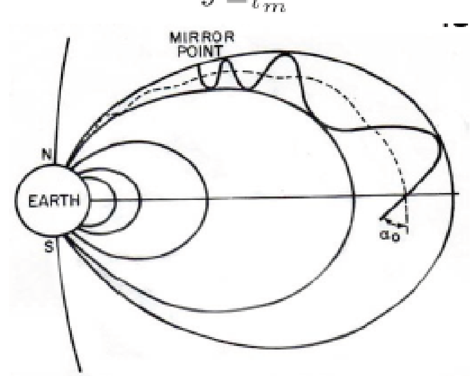

Drift motion:

- Gradient in magnetic field leads to drift motion around Earth: east for electrons, west for protons/ions
- period ~minutes
- associated 3rd invariant ϕ, magnetic flux:

$$\Phi = -\frac{2\pi B_E R_E^2}{L}$$

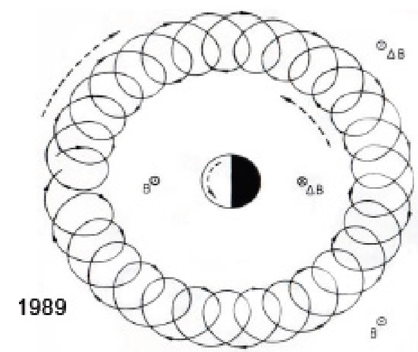

Trapped vs albedo components

Trajectories of all selected protons are propagated back and forth from the measurement location with no limit on tracing time/path

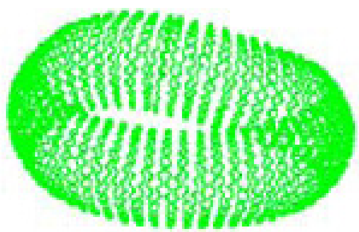

stably-trapped protons perform several drift cycles (>4) around the Earth without intercepting the absorbing atmosphere limit (40 km). In addition:

- ✓ They satisfy adiabatic conditions:

$$\omega_{gyro} >> \omega_{bounce} >> \omega_{drift}$$

- ✓ Results account for the breakdown of trapping at high energies (<4 GeV), as consequence of either large gyro-radius or non-adiabatic trajectory effects

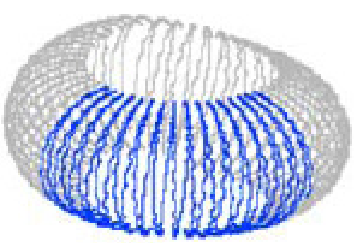

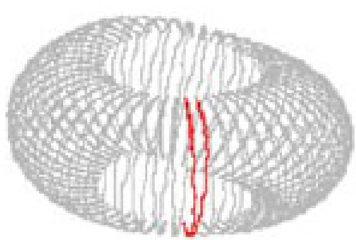

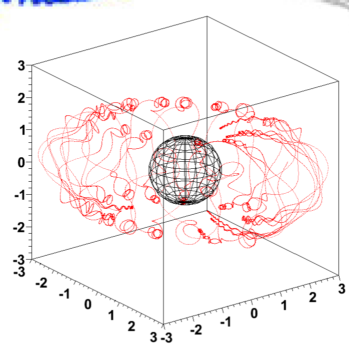

On the contrary, **albedo** proton trajectories intersect the atmosphere (40km), and can be classified into:

- **quasi-trapped** (trajectories similar to those of stably-trapped, but limited lifetimes)
- **un-trapped**, including a short-lived (precipitating) and a long-lived (pseudo-trapped or *penumbral*) components

Re-entrant albedo populations

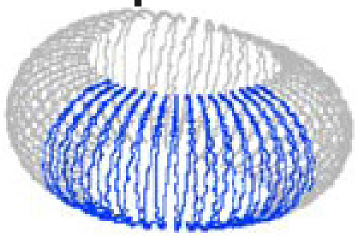

Lifetime = the time between the particle origin and its subsequent absorption in the atmosphere (40 km).

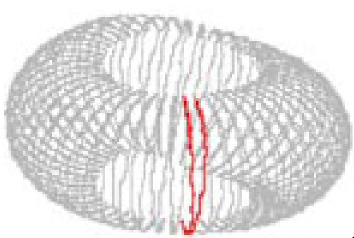

Since the quasi-trapped lifetime is of the order of a half drift period, which scales with ~ $1/\gamma\beta^2$, lifetime and energy have an approximately inverse proportional relation

Stormer vertical cutoff: $R=14.3/L^2$

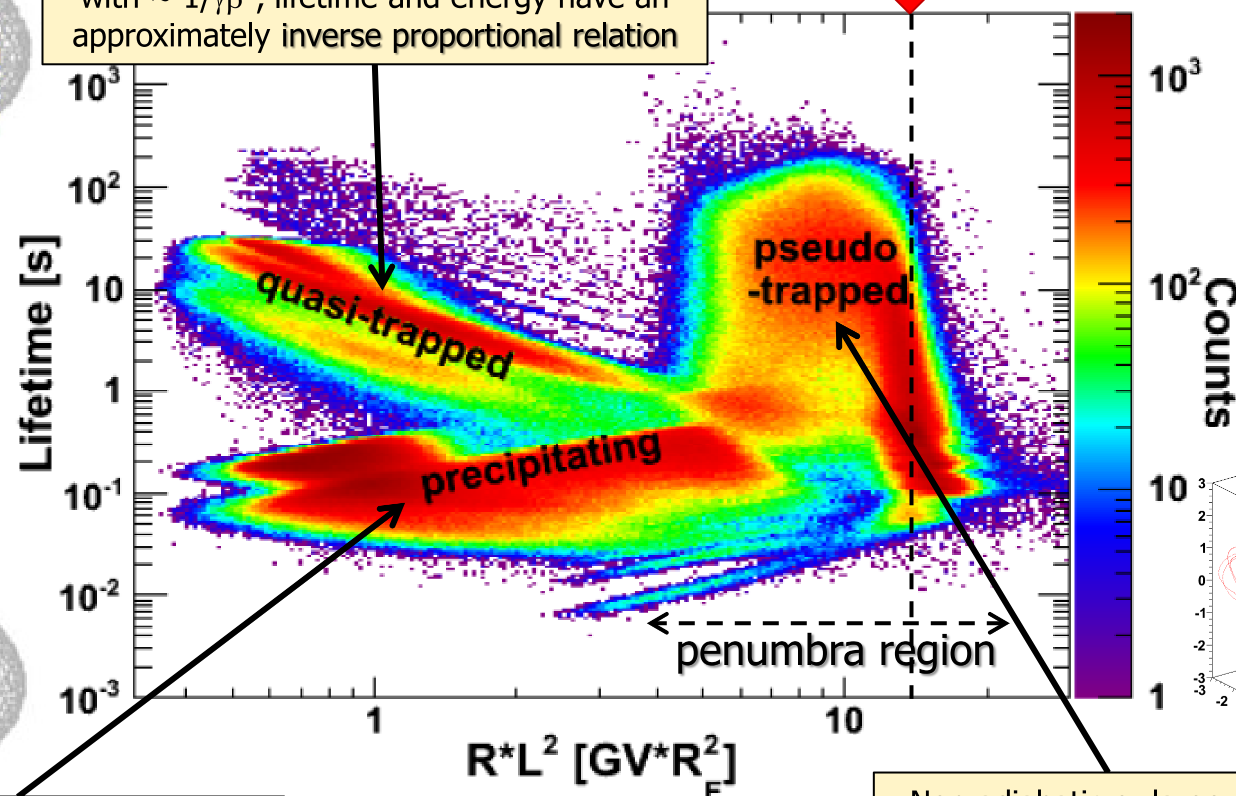

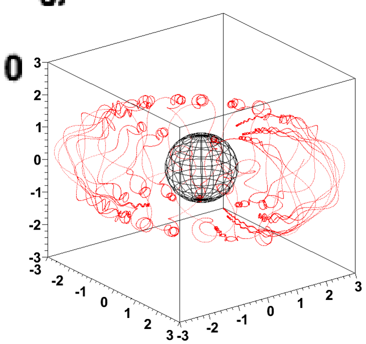

The precipitating lifetime is shorter than the typical bounce period, which scales with $1/\beta$, resulting in a weaker dependency on energy

Non-adiabatic or large gyro-radius effects cause the breakdown of (quasi) trapping conditions: irregular trajectories with no periodicity

Adriani et al., JGR – Space Physics, 120, 2015

Pitch-angle anisotropy

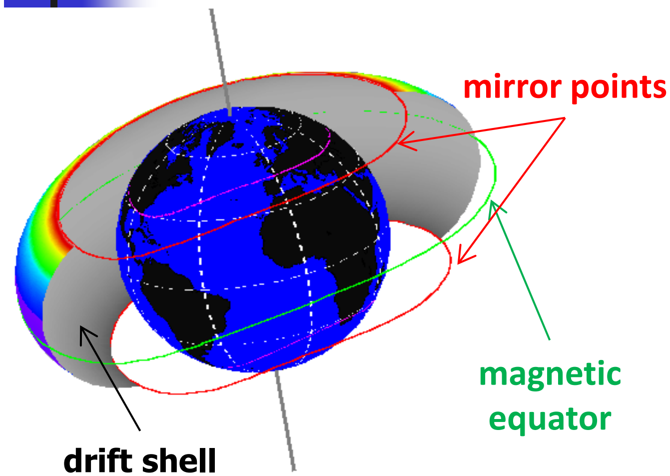

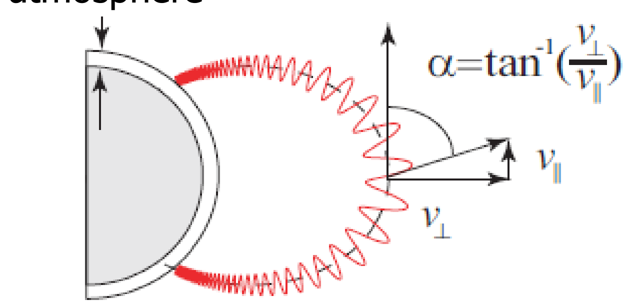

- Trapped fluxes in the SAA region are strongly anisotropic due to the interactions with the atmosphere
  - narrow pitch-angle distribution peaked at 90 deg equatorial pitch angle

- From the 1° adiabatic invariant conservation:

$$\frac{\sin^2\alpha}{B} = \frac{\sin^2\alpha_{eq}}{B_{eq}} = \frac{1}{B_m} = const$$

where B_m is the magnetic field at mirror points.

- The equatorial value α_{eq} is a convenient reference point.

Flux calculation
Differential directional fluxes

Flux intensities are properly estimated accounting for the flux anisotropic distribution (SAA)

- At former stage, proton fluxes are evaluated as a function of geographic position **X**=(Lon, Lat, Alt) and particle rigidity **R** and α pitch-angle with respect to the geomagnetic field:

$$F\left(\hat{X},R,\alpha\right)=\frac{N\left(\hat{X},R,\alpha\right)}{2\pi\sum_{\Psi\to\hat{X}}\left[H\left(\Psi,R,\alpha\right)\cdot\Delta T\left(\Psi\right)\right]\cdot\Delta R}$$

proton counts corrected by selection efficiencies

sum over satellite orientations Ψ at geographic position **X**

livetime spent by PAMELA at each spacecraft orientation Ψ

PAMELA's effective area

$$H\left(R,\alpha\right)=\frac{\sin\alpha}{2\pi}\int_0^{2\pi}d\beta\left[A\left(R,\vartheta,\varphi\right)\cos\vartheta\right]$$

evaluated with MC methods

apparatus response function

- The relationship between local (ϑ,φ - PAMELA frame) and magnetic (α,β) angles describing particle direction, depends on the satellite orientation Ψ with respect to the geomagnetic field.
- PAMELA's effective area is rigidity dependent due to the bending effect of the magnetic spectrometer.
- **<u>No assumption on α distribution is done</u> (e.g. by using sampling fuctions such as $sin^n\alpha$)**

Finite gyro-radius effects

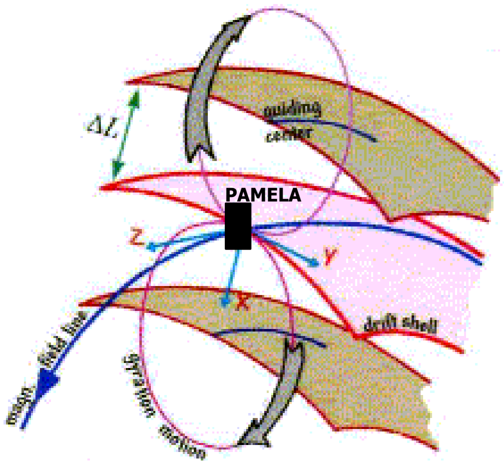

- Finite gyro-radius effects are not negligible at PAMELA energies
  - Gyro-radius of tens/hundreds km, depending on magnetic field intensity and proton energy
  - Guiding line approximation no longer valid for higher energies
    - the spatial scale of the magnetic field is not much smaller than the gyro-radius
  - East-West effect
    - Relatively small in our data due to PAMELA small aperture, and since PAMELA vertical axis is mostly directed towards the zenith

✓ Consequently, measured flux intensities are shifted to the corresponding guiding center locations

Flux calculation
Differential directional fluxes

$F(\mathbf{X},\alpha,E)$

geographic grid

$\mathbf{X}$=(Lat,Lon,Alt)

East-West effect correction

$F(\mathbf{X}_{GC},\alpha,E)$

$\mathbf{X}_{GC}$=guiding center positions

interpolation

$F(\mathbf{K},\Phi,E)$

invariant coordinates

1)adiabatic invariants $\mathbf{K},\Phi$

2)Roeder/McIlwain **L**-shell vs eq. pitch angle

3)invariant altitude vs magnetic latitude

Flux results
Geographic Maps

Adriani et al., ApJL 791:L4, 2015

columns: same energy bins
rows: same altitude bins

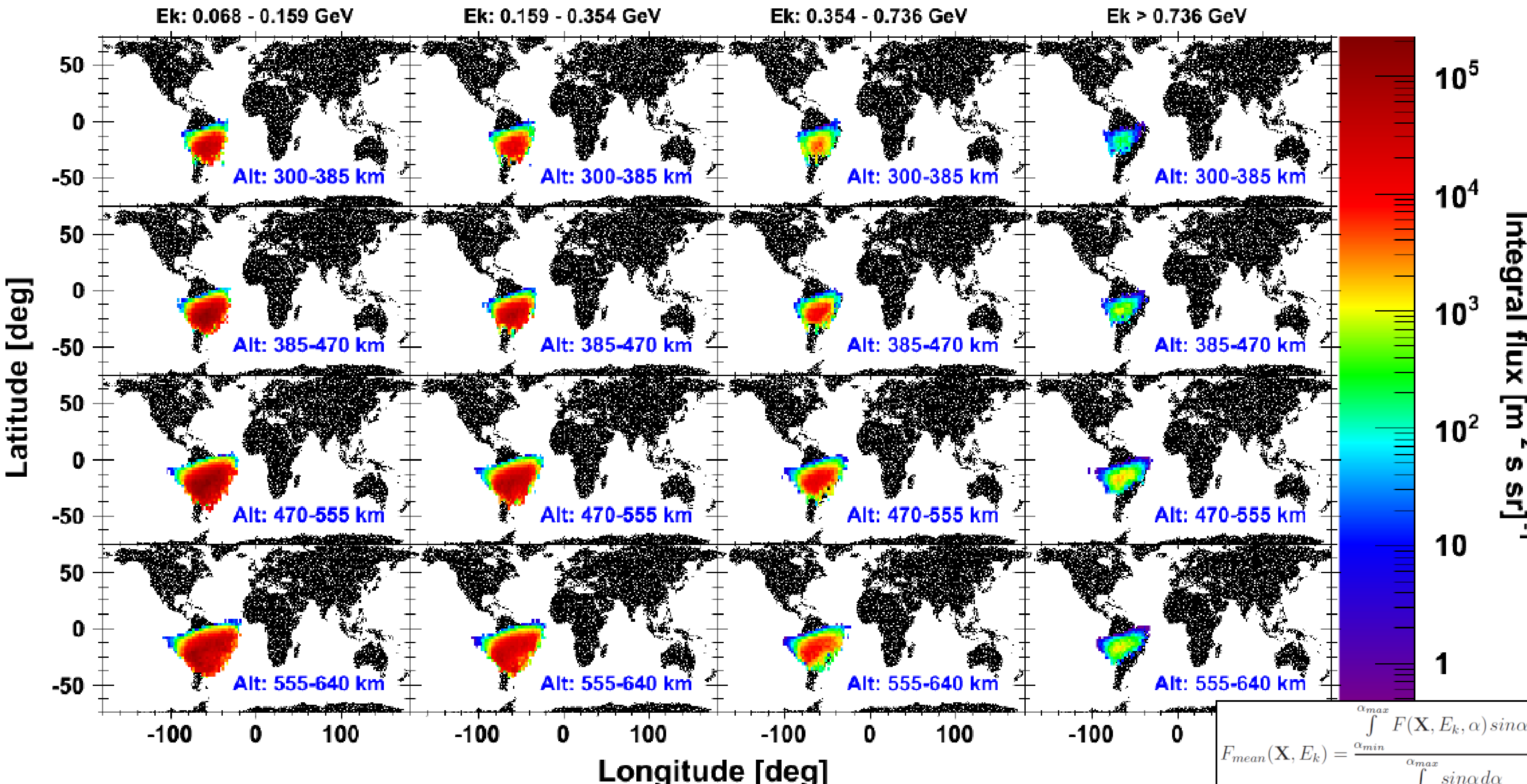

$$F_{mean}(\mathbf{X}, E_k) = \frac{\int_{\alpha_{min}}^{\alpha_{max}} F(\mathbf{X}, E_k, \alpha)\, sin\alpha\, d\alpha}{\int_{\alpha_{min}}^{\alpha_{max}} sin\alpha\, d\alpha}$$

Stably-trapped integral flux ($m^{-2}s^{-1}sr^{-1}$) averaged over the pitch angle range covered by PAMELA, as a function of geographic coordinates, evaluated for different energy (columns) and guiding center altitude (rows) bins.

Flux results
Adiabatic invariants

Adriani et al., ApJL 791:L4, 2015

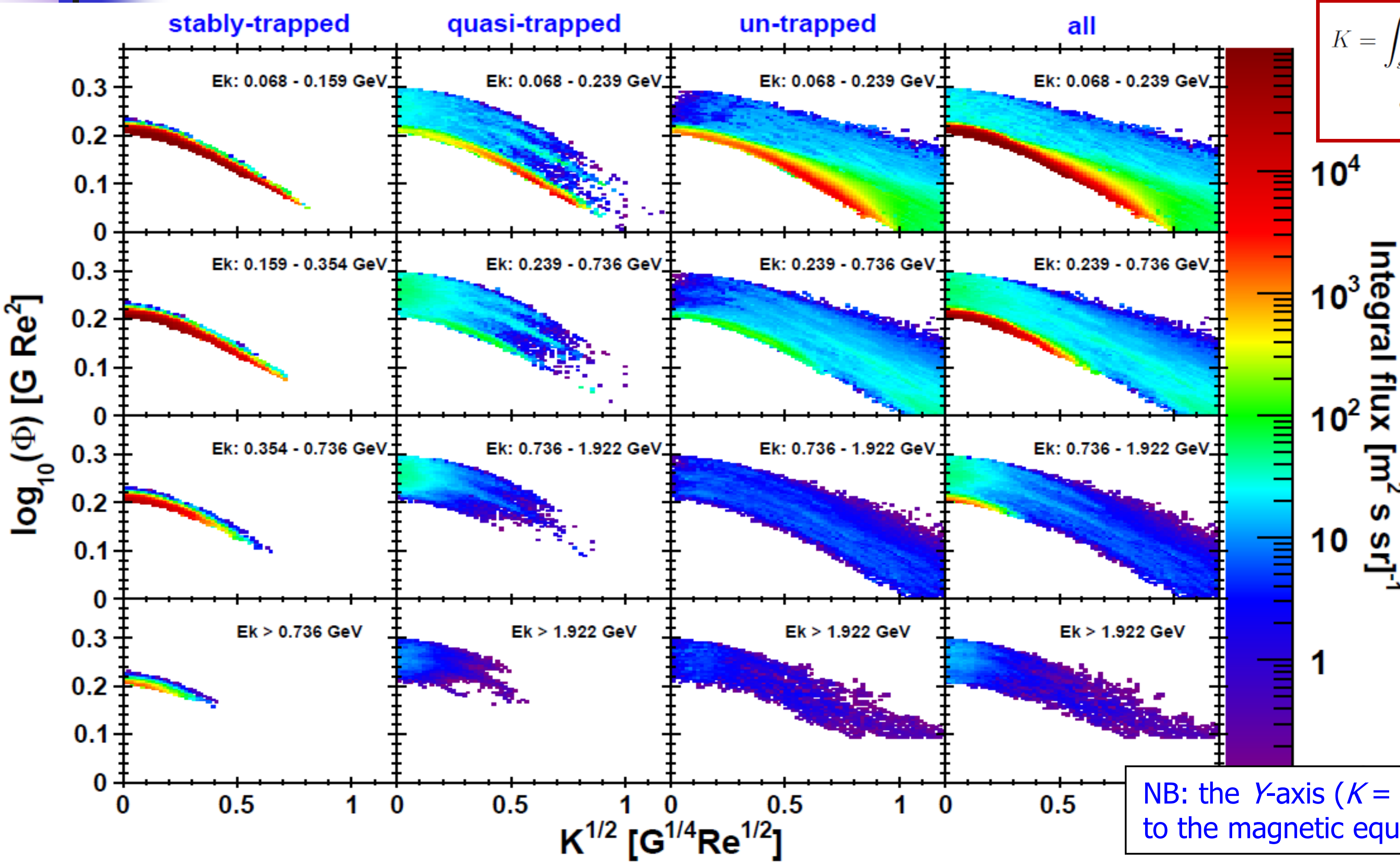

$$K = \int_{s_m}^{s'_m} [B_m - B(s)]^{1/2} ds$$

$$\Phi = \oint \mathbf{A} \cdot \mathbf{dl}$$

NB: the *Y*-axis (*K* = 0) corresponds to the magnetic equator

Proton integral fluxes ($m^{-2}s^{-1}sr^{-1}$) as a function of the second *K* and the third Φ adiabatic invariant, for different kinetic energy bins (see the labels).
Results for the different populations are reported (from left to right): stably-trapped, quasi-trapped, un-trapped and the total under-cutoff proton sample.

Flux results

Equatorial pitch angle vs L-shell

Adriani et al., ApJL 791:L4, 2015

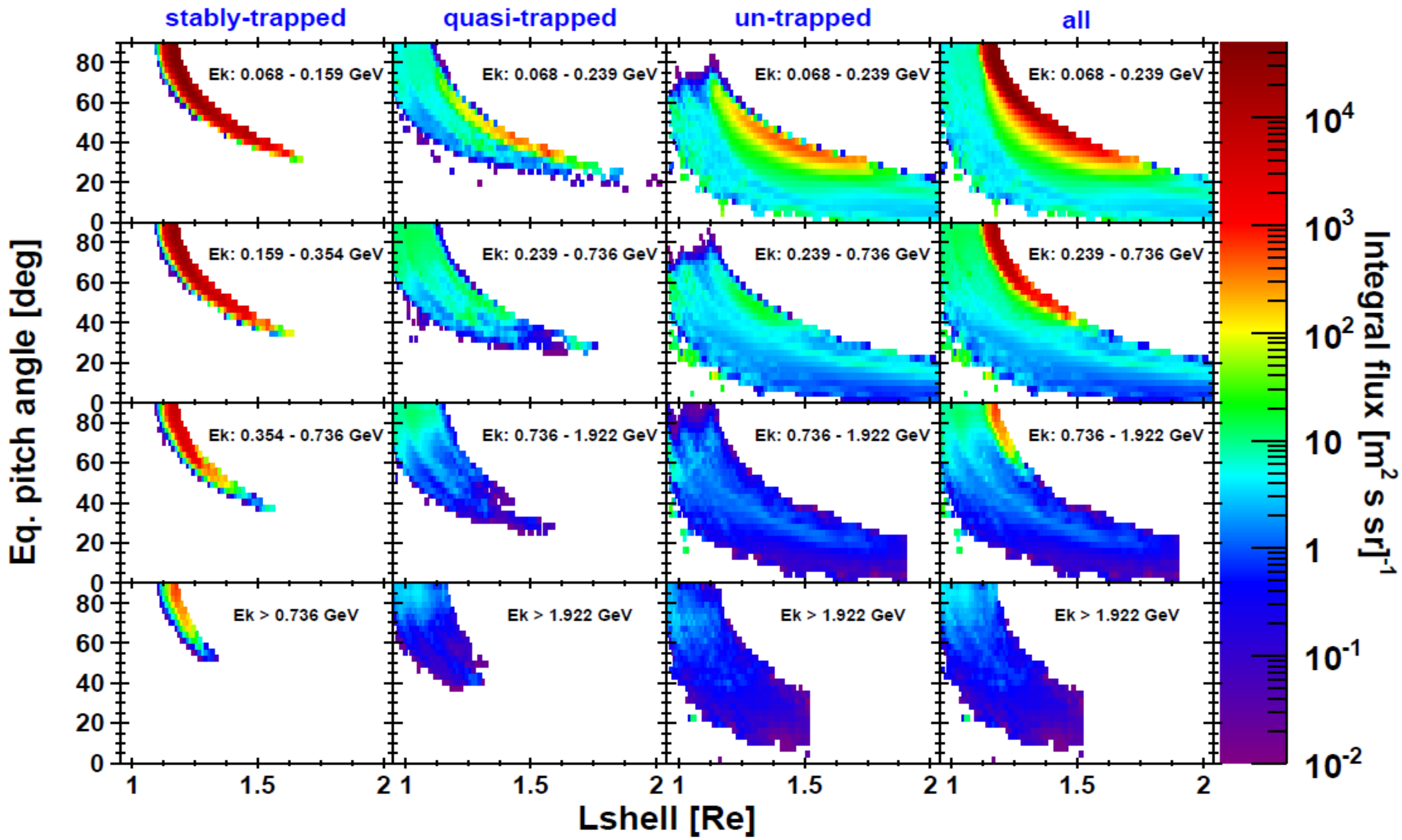

Proton integral fluxes ($m^{-2}s^{-1}sr^{-1}$) as a function of equatorial pitch angle and McIlwain's *L*-shell, for different kinetic energy bins (see the labels).
Results for the different populations are reported (from left to right): stably-trapped, quasi-trapped, un-trapped and the total under-cutoff proton sample.

Trapped fluxes

Comparison with semi-emphirical models

Adriani et al., ApJL 791:L4, 2015

Stably-trapped differential fluxes (GeV^{-1}m^{-2}s^{-1}sr^{-1}) compared with predictions from **AP8-min** (Sawyer & Vette 1976) and **PSB97** (Heynderickx et al. 1999) semi-empirical models, denoted with dashed black line and the solid blue line respectively. Model calculations from the SPENVIS on-line system (Heynderickx et al. 2000).

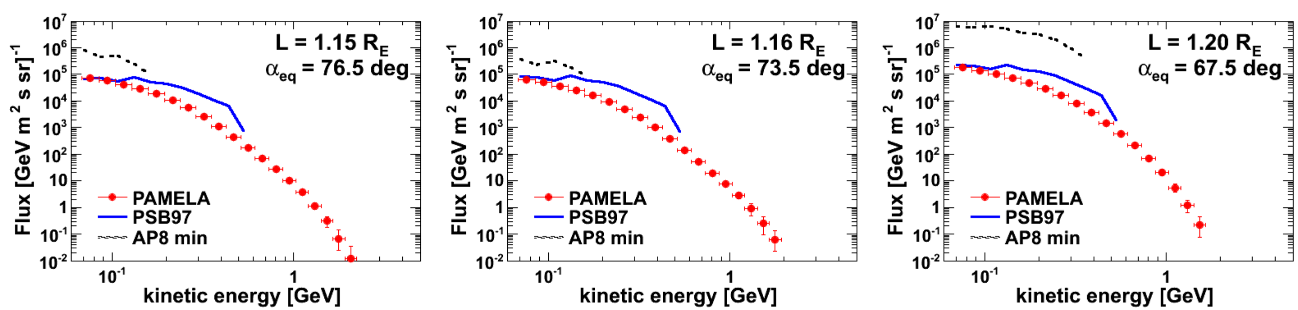

sample energy spectra for three combinations of equatorial pitch angle and McIlwain's L-shell

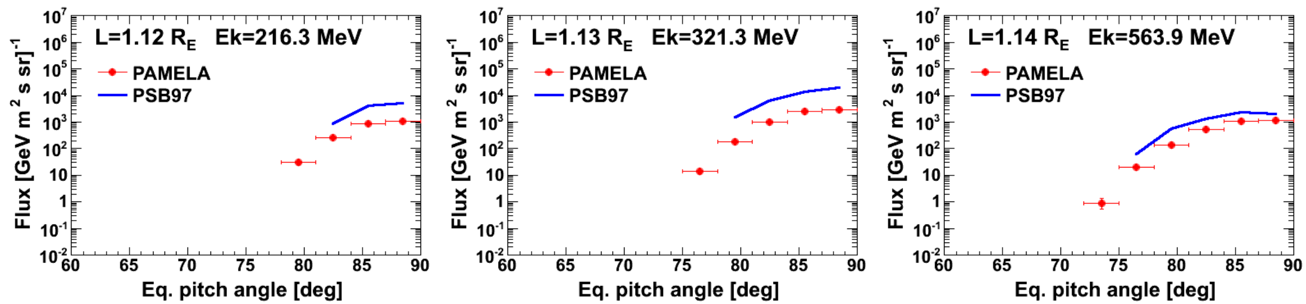

equatorial pitch angle profiles for three combinations of kinetic energy and L-shell values

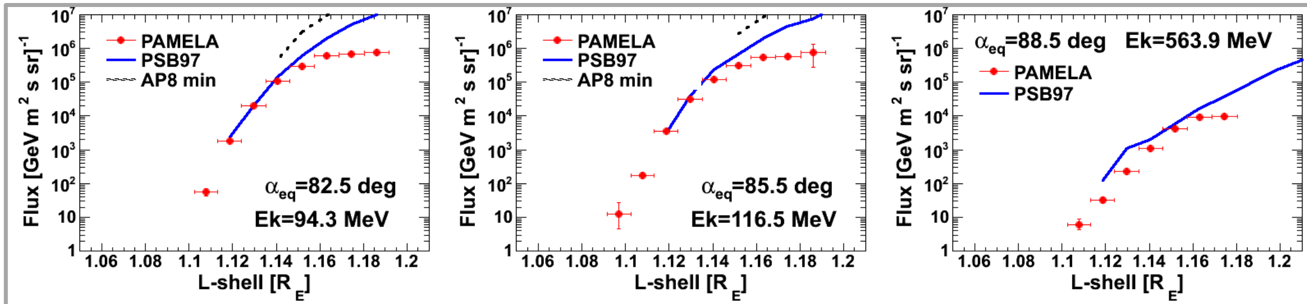

L-shell profiles for three combinations of kinetic energies and equatorial pitch angles.

Trapped fluxes

Preliminary comparison with AP9

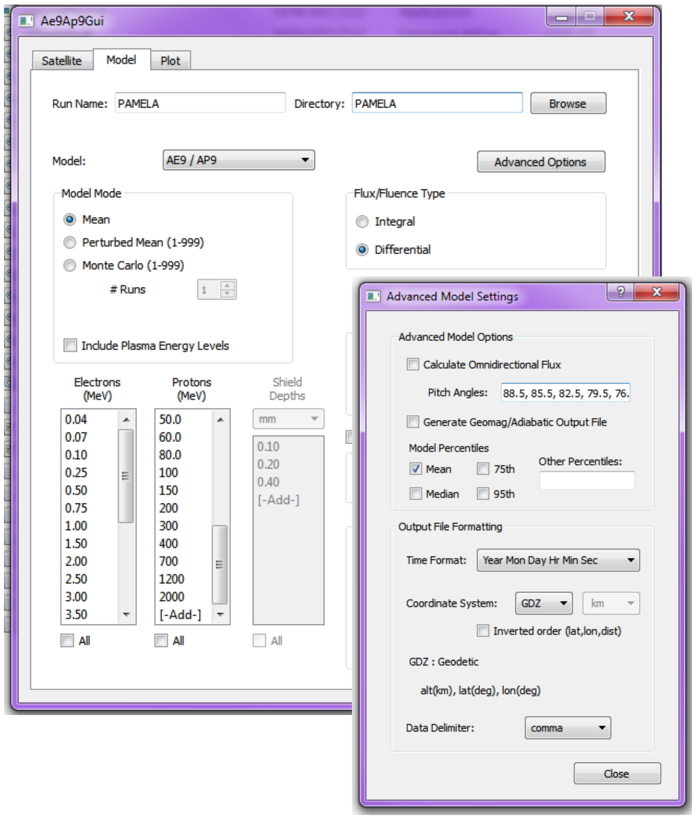

Ae9Ap9_version_1.20.003 (Windows)
https://www.vdl.afrl.af.mil/programs/ae9ap9

Fluxes estimated over a 5-dimensional grid:
- Lat, Lon, Alt, E, and local pitch angle α

Same binning used for the PAMELA fluxes

Energy integrated intensities based on **geographic coordinates** are evaluated by averaging the directional fluxes over the full/ available local pitch angle range

NB: the limited pitch-angle coverage of PAMELA must be taken into account when comparing with other data sets

Trapped fluxes

Preliminary comparison with AP9

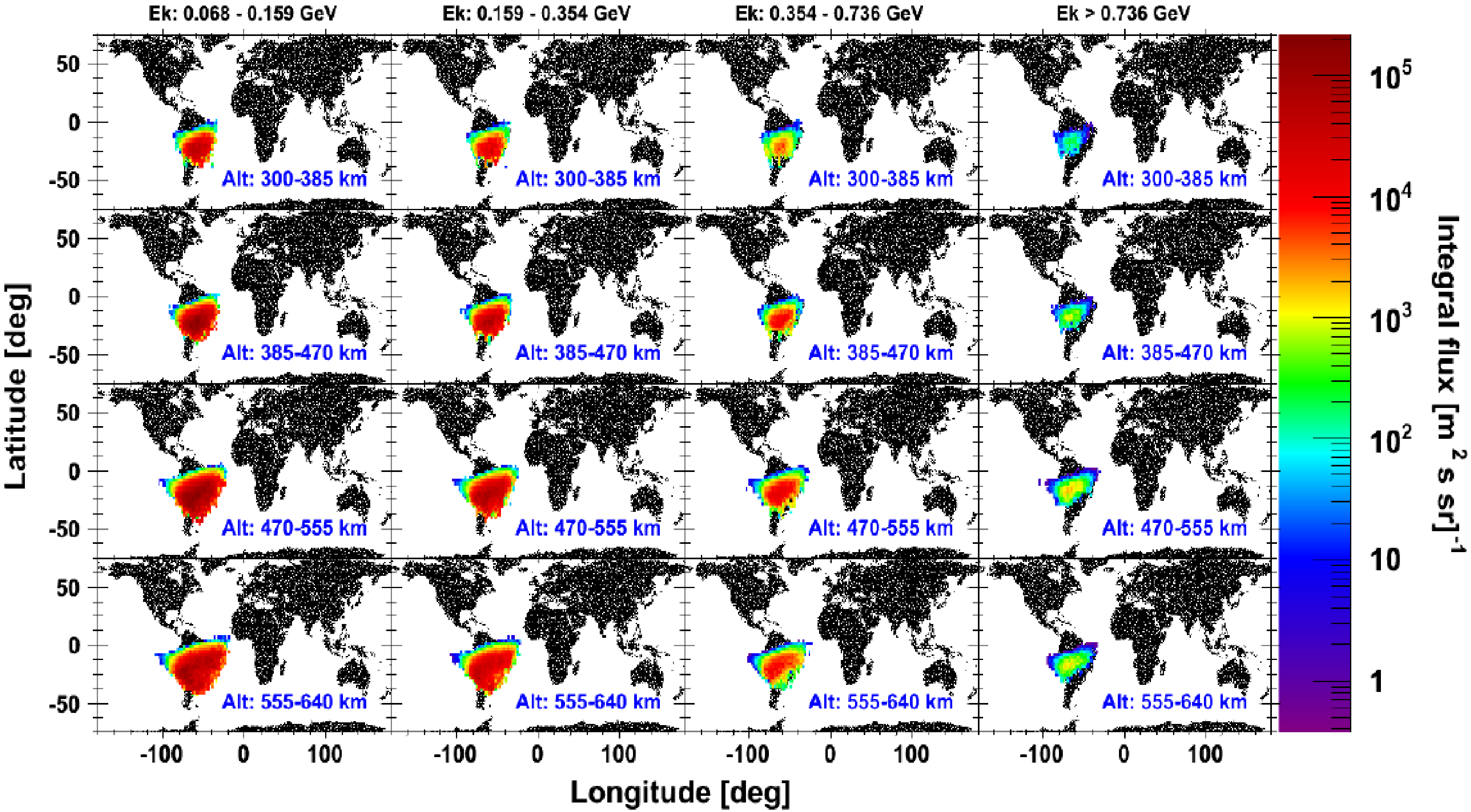

Pitch-angle averaged fluxes measured by PAMELA

Trapped fluxes

Preliminary comparison with AP9

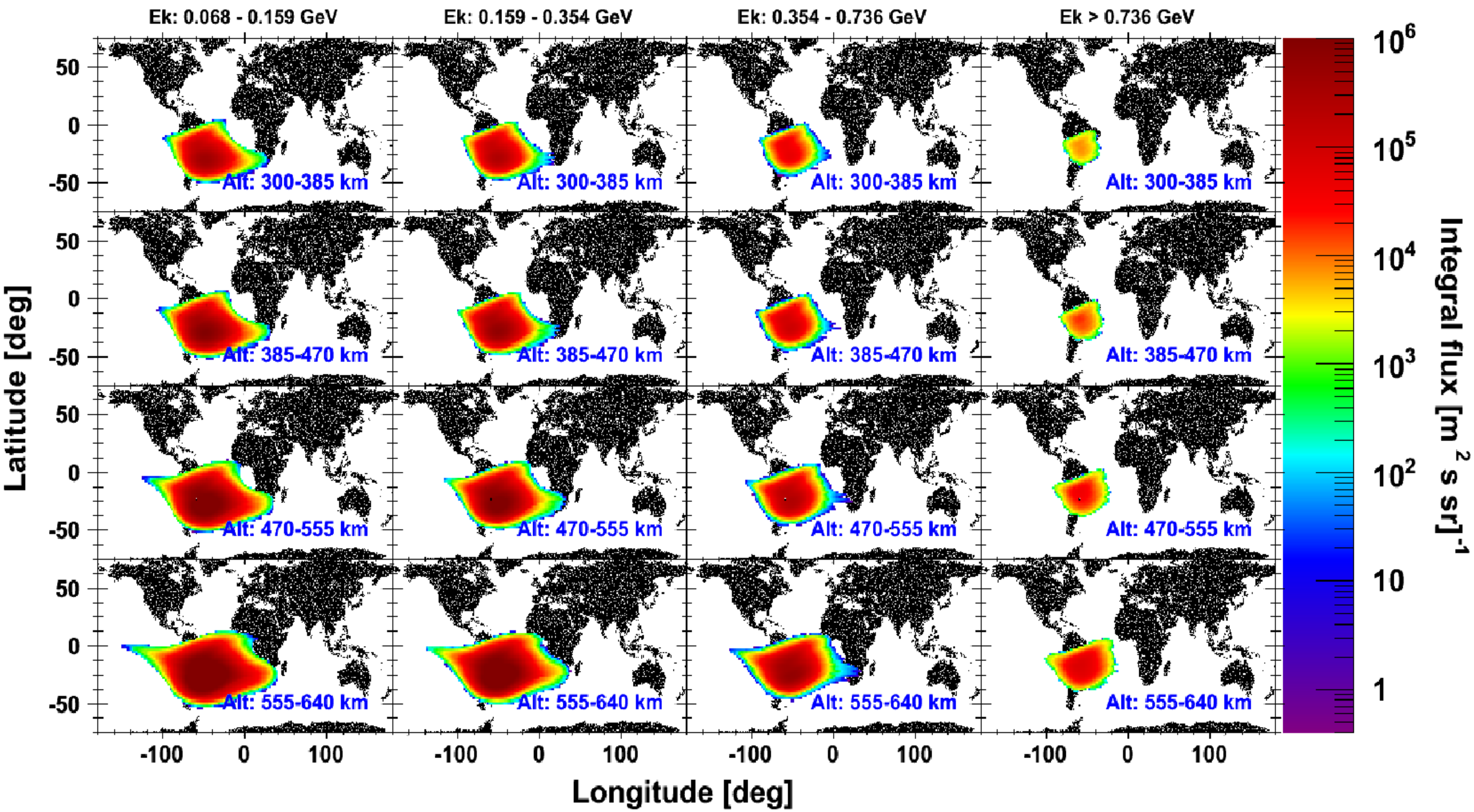

AP9 fluxes averaged over the local pitch-angle range 0-180 deg

Trapped fluxes
Preliminary comparison with AP9

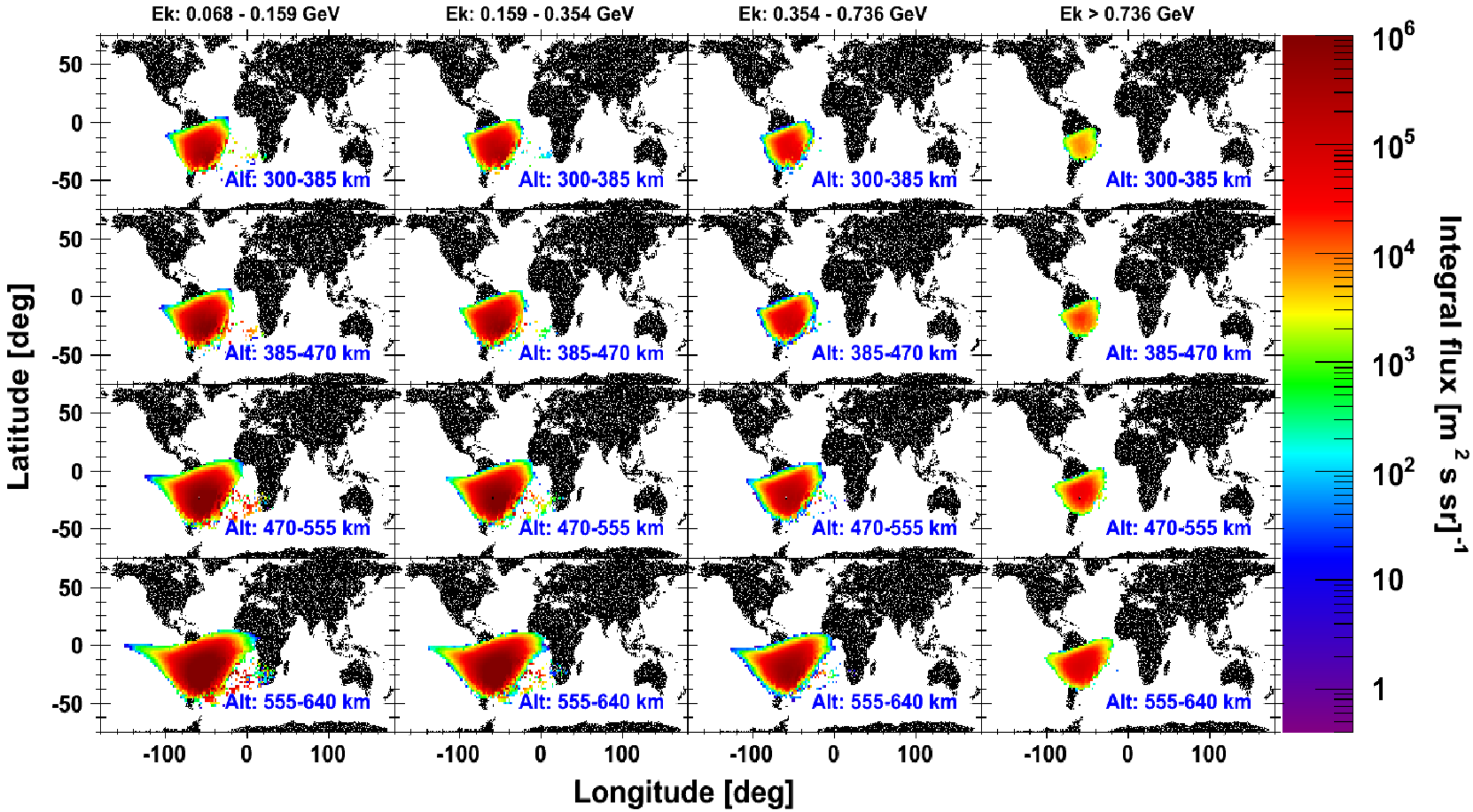

AP9 fluxes averaged over the local pitch-angle range available to PAMELA

Trapped fluxes

Preliminary comparison with AP9

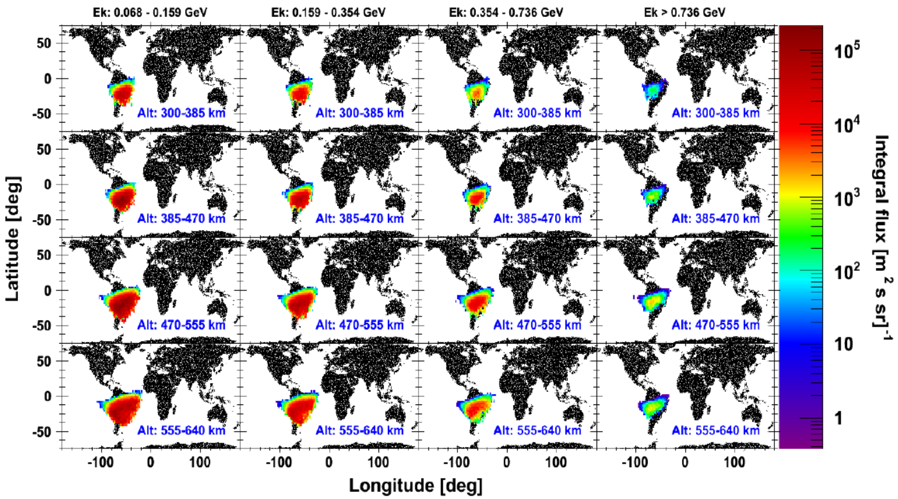

Pitch-angle averaged fluxes measured by PAMELA

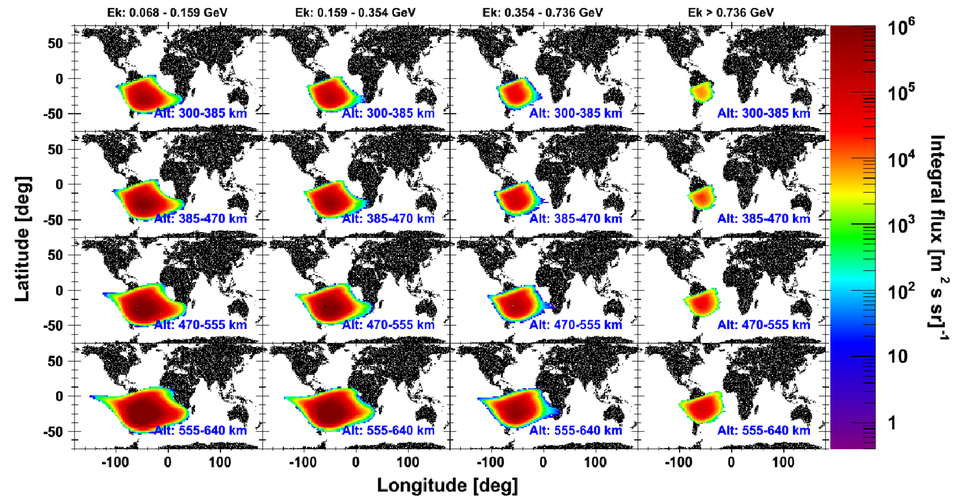

AP9 fluxes averaged over the local pitch-angle range 0-180 deg

In general PAMELA and AP9 fluxes have quite similar distributions, but AP9 mean intensities are about 1 order of magnitude larger than PAMELA ones. The discrepancy increases up to 2 orders of magnitude at highest kinetic energies, where AP9 results are obtained through model extrapolation.

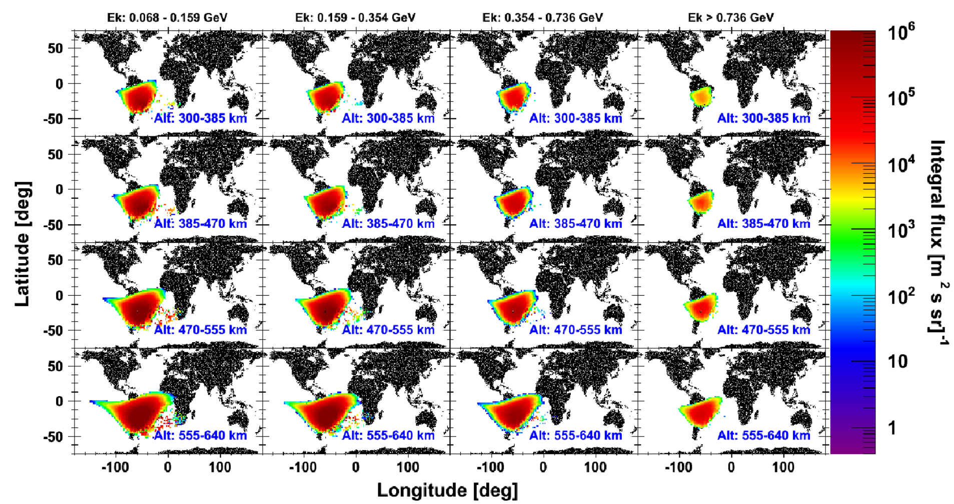

AP9 fluxes averaged over the local pitch-angle range available to PAMELA

Trapped fluxes

Comparison with theoretical models

Adriani et al., ApJL 791:L4, 2015

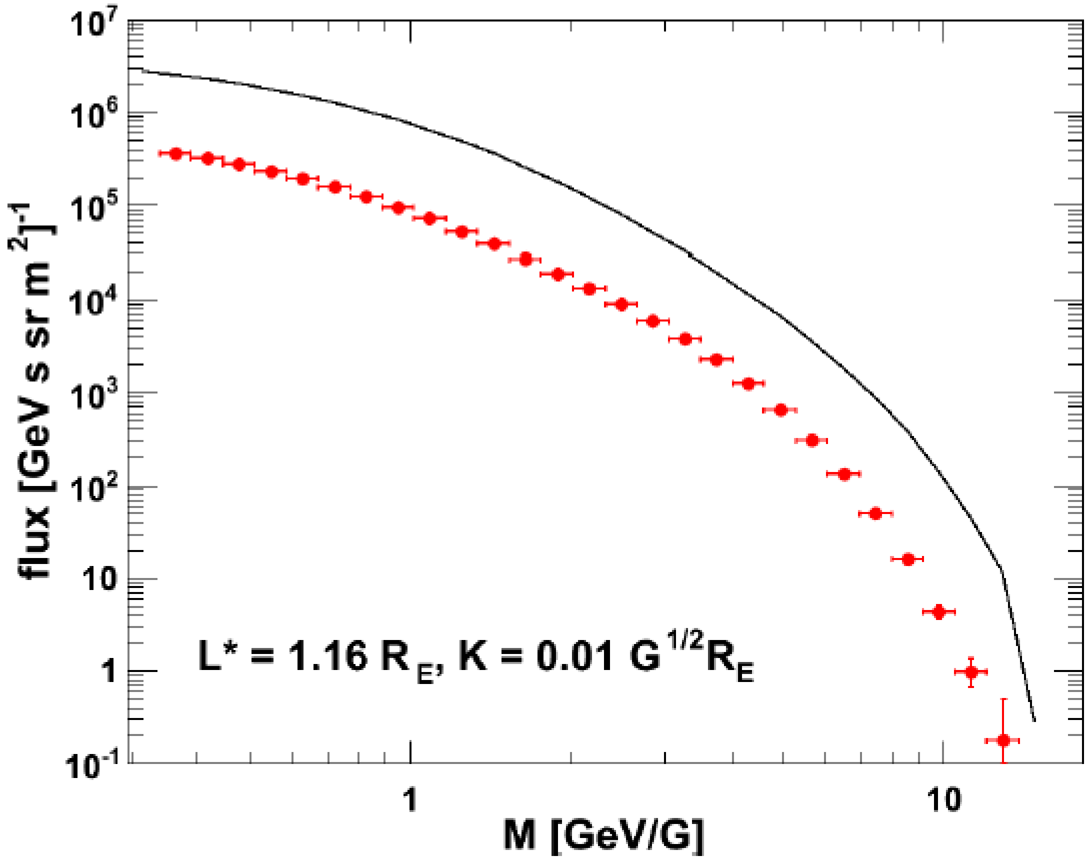

$$L^* = \frac{2\pi \mu_E}{R_E \Phi}$$

Stably-trapped differential flux (GeV^{-1}m^{-2}s^{-1}sr^{-1}) at geomagnetic equator compared with the calculation by **Selesnick et al. (2007)** for the year 2000. Spectra are reported as a function of the 1st adiabatic invariant M, for sample values of K (2nd adiabatic invariant) and L* (Roeder's parameter) invariants.

Re-entrant albedo spectra

Differential energy spectra outside the SAA region measured for different bins of magnetic latitude (see the labels).

Results for the different proton populations are shown: quasi-trapped (**blue**), precipitating (**green**), pseudo-trapped (**red**) and interplanetary (**black**).

Adriani et al., JGR – Space Physics, 120, 2015

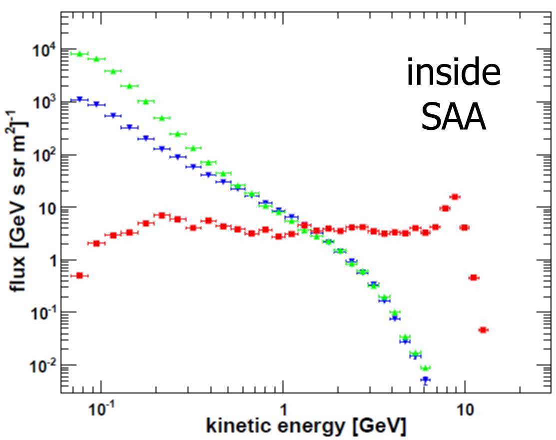

Differential energy spectra in the **SAA** region (B<0.23 G)

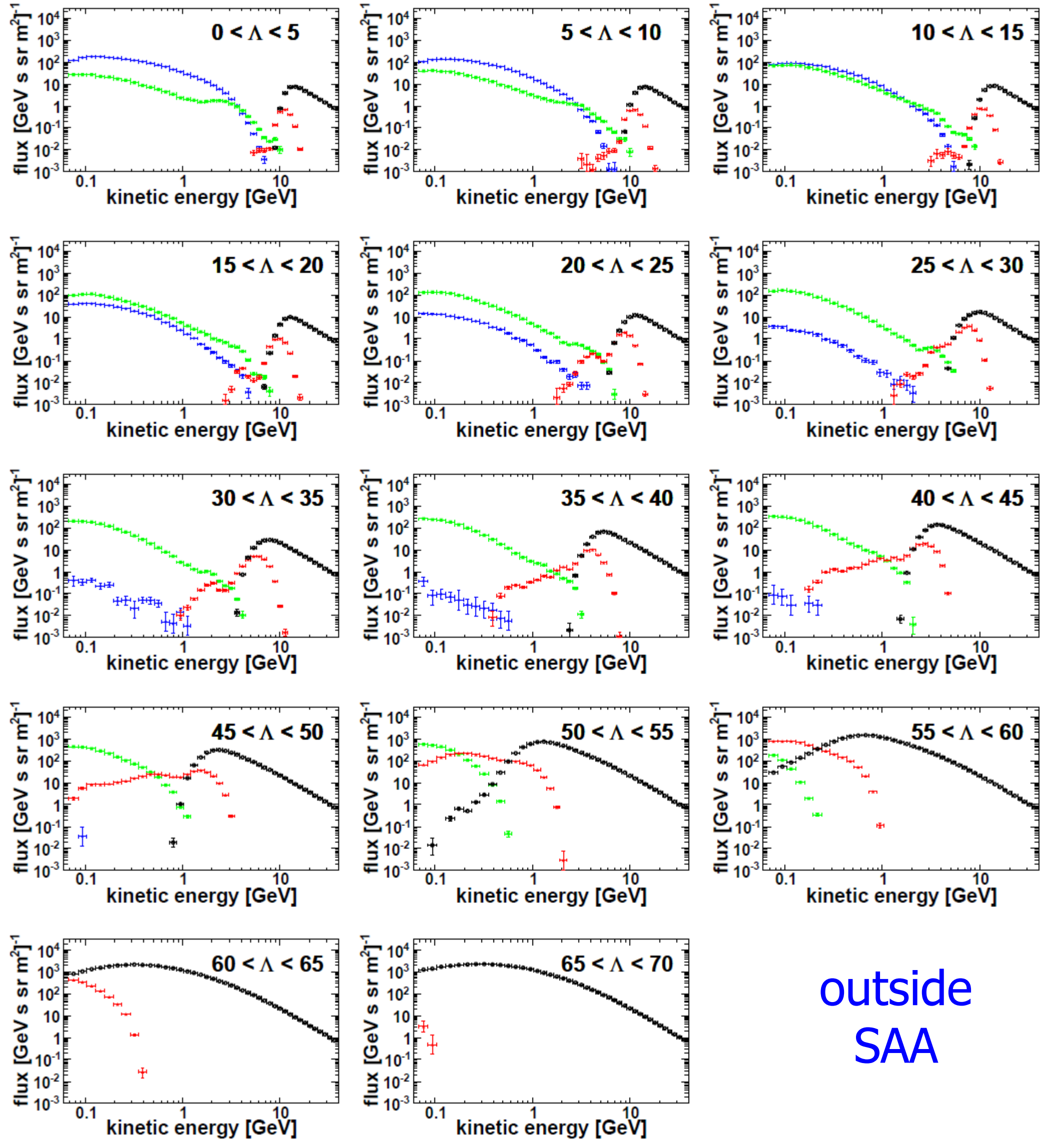

The discovery of geomagnetically trapped antiprotons

Adriani et al., ApJL, 737:L29, 2011

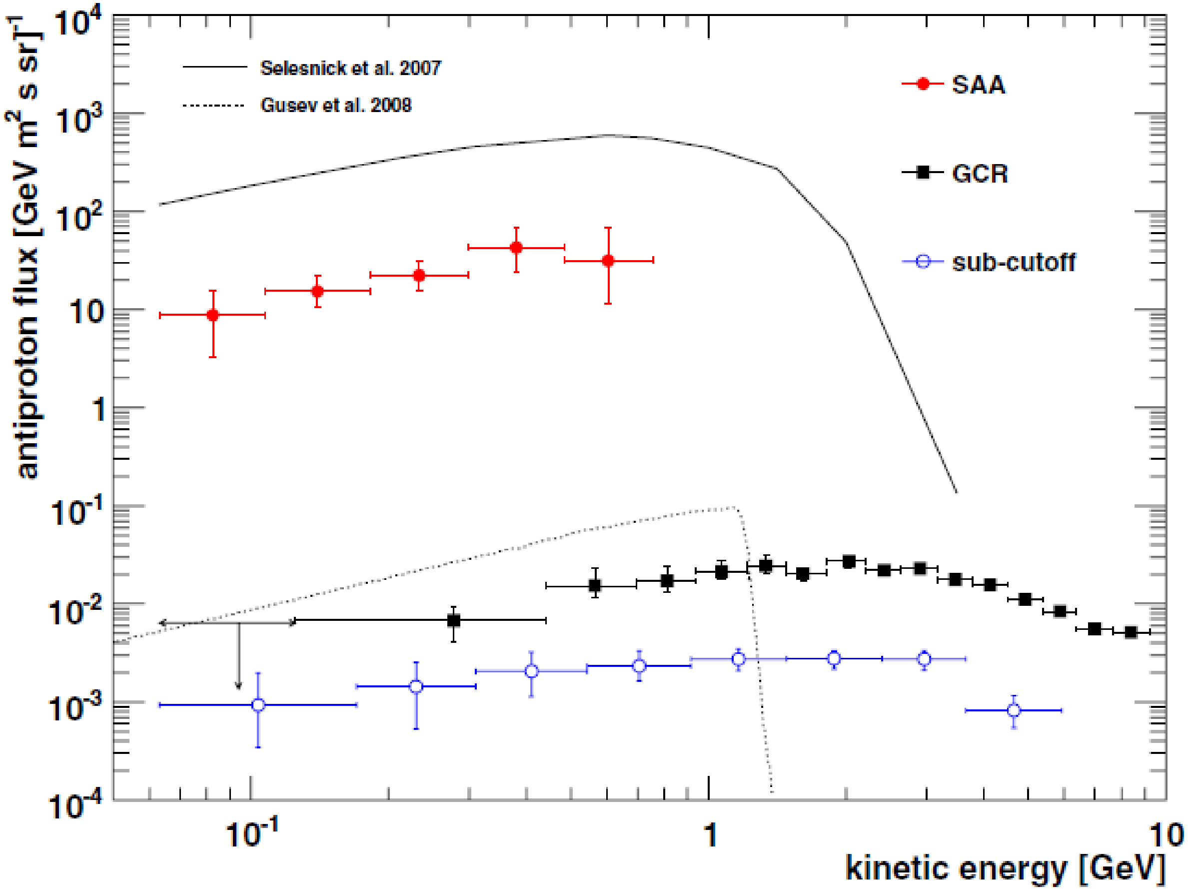

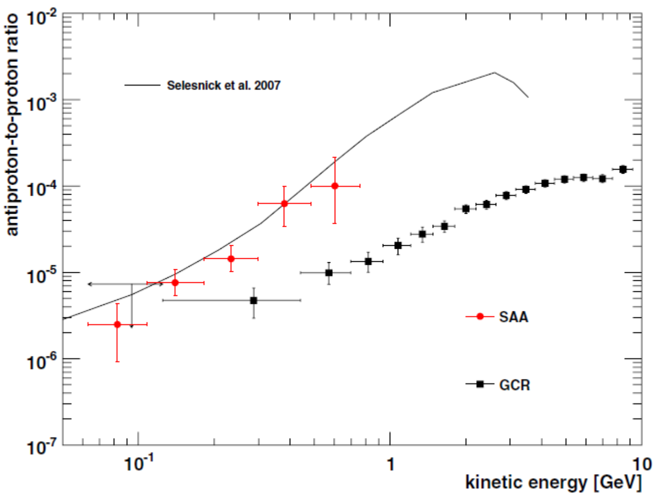

pbar/p ratio in the SAA

Similar to trapped protons, trapped antiprotons are mainly produced by the decay of albedo antineutrons (CRANbarD mechanism, Selesnick et. al. (2007))

PAMELA & Space Weather

solar cycles 23 and 24

- Measurement of Solar Energetic Particle (SEP) events
  - first direct measurement of ~relativistic SEP spectra
  - first direct measurement of SEP angular distributions
  - cross-calibration of the GOES proton detectors (EPEAD/HEPAD)
- Investigation of geomagnetic effects during magnetospheric storms induced by large CME events
  - direct measurement of the related geomagnetic cutoff variations
- Measurement of particle-dependent solar modulation effects
- Measurement of Forbush decrease effects
- Studies related to Corotating Interaction Regions (CIRs), etc.

Solar energetic particle events

Investigation of flux anisotropy

Adriani et al., ApJL 801:L3, 2015

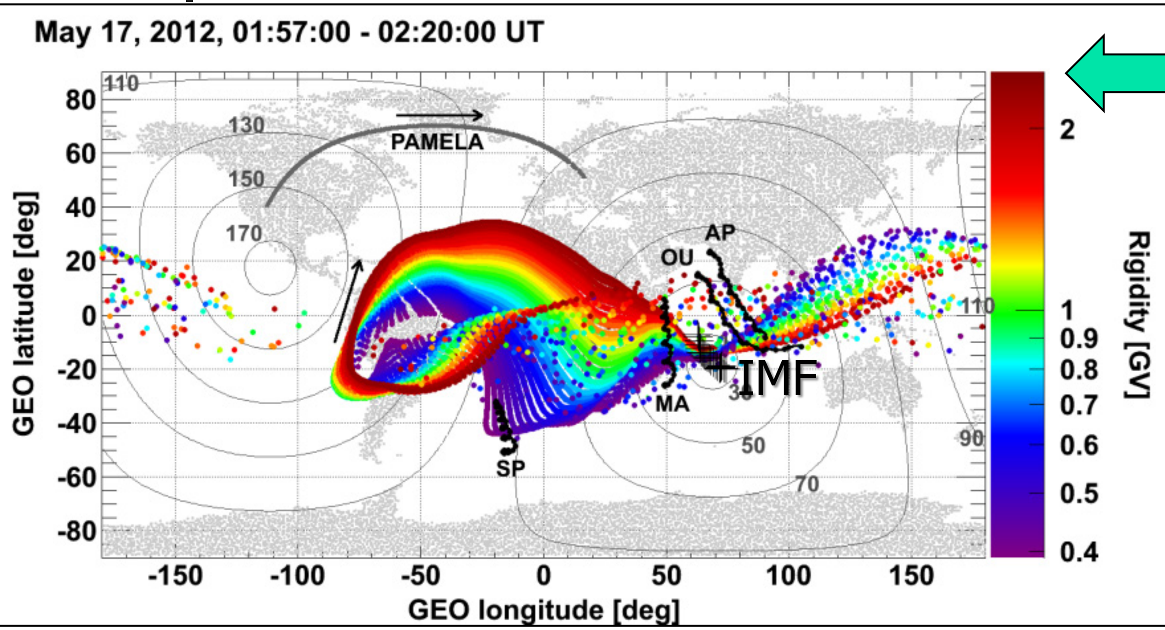

asymptotic directions of view of PAMELA during the first polar pass that registered the 17 May 2012 GLE

Adriani et al., ApJ, 801:L3, 2015

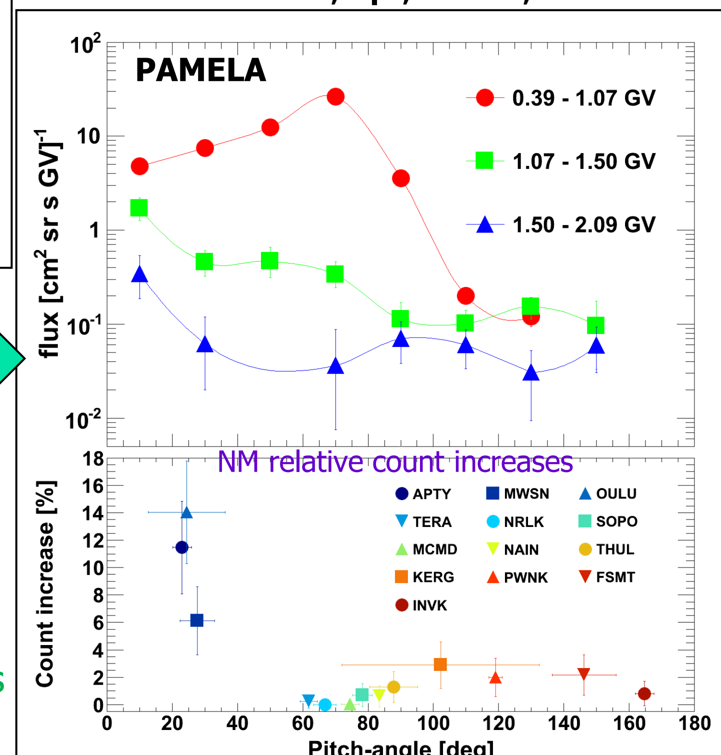

pitch-angle profiles for different rigidity bins

PAMELA observes two populations simultaneously with very different pitch angle distributions:

a low-energy component (<1 GV)

- confined to pitch angles<90°, with significant scattering/redistribution;

and a high-energy component (>1.5 GV)

- beamed with pitch angles <30°, consistent with NM observations.

The component with intermediate energies (1 - 1.5 GV) suggests a transition between the low and high energies.

Geomagnetic effects

the 14 Dec 2006 magnetospheric storm

Data missing from 10:00 UT on Dec 13 until 09:14 UT on Dec 14 because of an onboard system reset of the satellite

Time profile of the geomagnetic cutoff latitudes measured by PAMELA for different rigidity bins

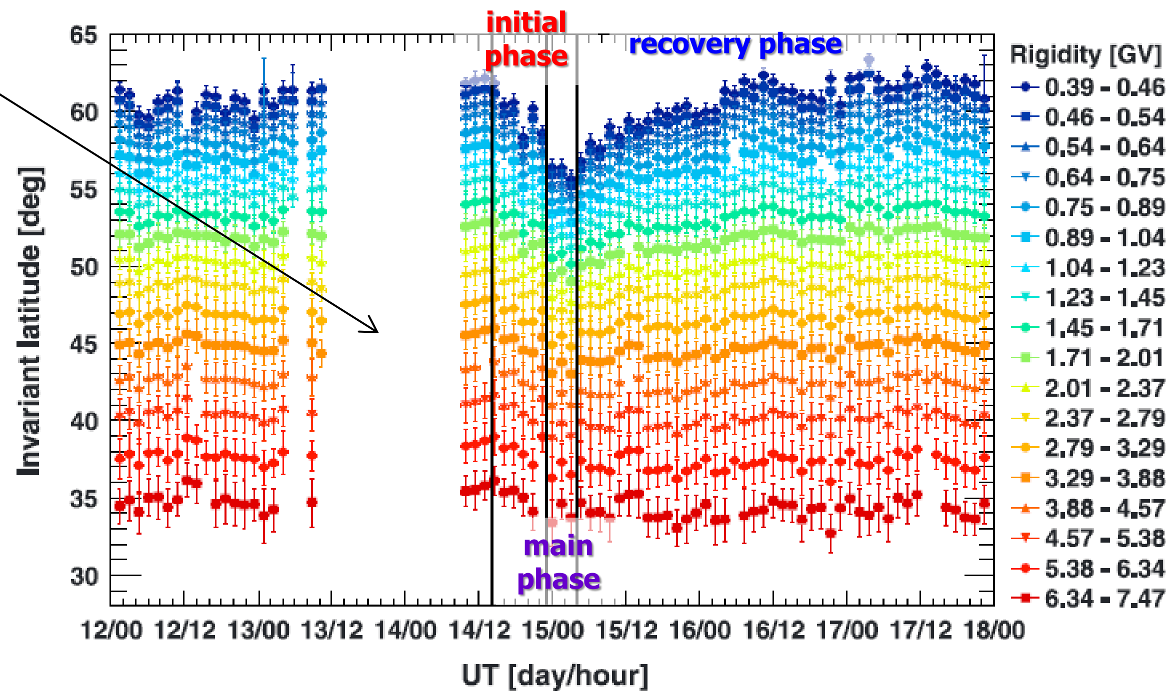

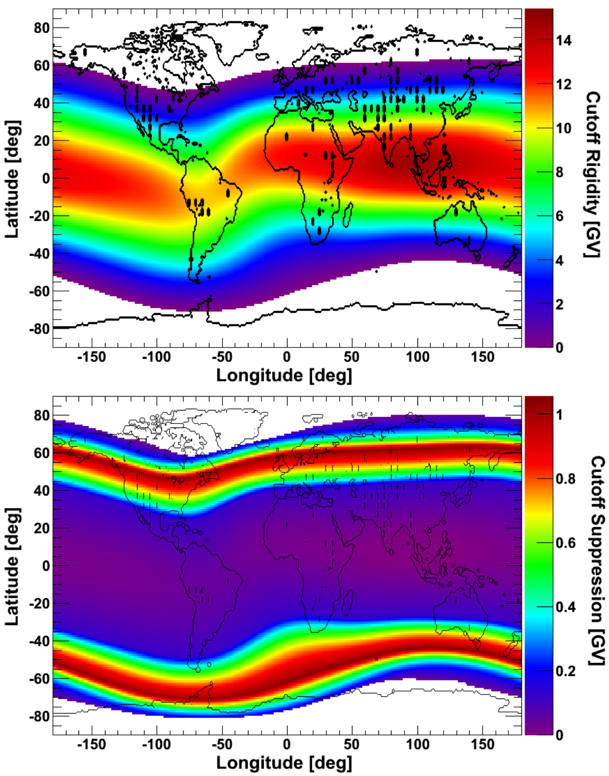

cutoff map at time of maximum suppression

The evolution of the magnetic storm followed the typical scenario in which the cutoff latitudes move equatorward as a consequence of a CME impact on the magnetosphere with an associated transition to southward IMF B_z.

Adriani et al., Space Weather, 14, 2006

Summary & conclusions

- The low-altitude proton population was analyzed and classified into geomagnetically trapped and albedo (quasi-trapped, un-trapped) components.

- Flux anisotropies were properly taken into account, by evaluating the instrument directional response as a function of the spacecraft orientation with respect to the local geomagnetic field.

- Maps of high-energy (>70 MeV) proton fluxes were provided, by using both geographical and adiabatic invariants coordinates.
  - PAMELA results improve the description of the trapped protons at lower altitudes (down to L~1.1 R_E) and at higher energies (up to E~4 GeV), where current models suffer from large uncertainties.

- Results were compared with the predictions of the theoretical and empirical proton models available in the same energetic region (AP8, PSB-97, AP9).

Future developments

- Analysis of trapped proton data acquired by PAMELA after September 2009
- Analysis of magnetospheric electrons, positrons and light nuclei
- Development of a **PAMELA model** for the high-energy radiation at low Earth orbits
  - intepolation, smoothing algorithm, related uncertainties, etc.
  - extrapolation of measured fluxes in the phase-space region not covered by PAMELA (e.g. extrapolatation of the pitch-angle fluxes to the equator for the higher L-shells)

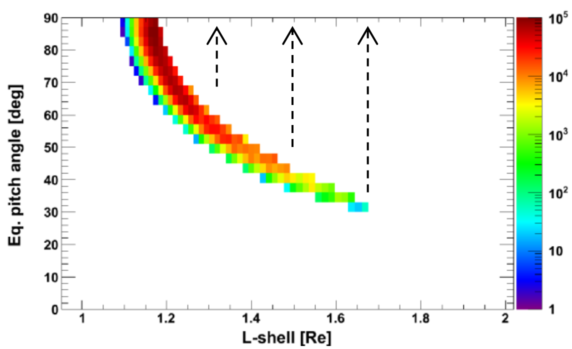

References

- O. Adriani et al. (2011), *The discovery of geomagnetically trapped cosmic-ray antiprotons*. In: Astrophysical Journal Letters 737.2. doi: 10.1088/2041-8205/737/2/L29.
- O. Adriani et al. (2014), *The PAMELA Mission: Heralding a new era in precision cosmic ray physics*. In: Physics Reports 544.4, pp. 323-370. doi:10.1016/j.physrep.2014.06.003.
- O. Adriani et al. (2015), *Trapped proton fluxes at low earth orbits measured by the PAMELA experiment*. In: Astrophysical Journal Letters 799.1. doi: 10.1088/2041-8205/799/1/L4.
- O. Adriani et al. (2015), *Reentrant albedo proton fluxes measured by the PAMELA experiment*. In: Journal of Geophysical Research A: Space Physics 120.5, pp. 3728-3738. doi: 10.1002/2015JA021019.
- O. Adriani et al. (2015), *PAMELA's measurements of magnetospheric effects on high-energy solar particles*. In: Astrophysical Journal Letters 801.1. doi: 10.1088/2041-8205/801/1/L3.
- O. Adriani et al. (2016), *PAMELA's measurements of geomagnetic cutoff variations during the 14 December 2006 storm*. In: Space Weather 14.3, pp. 210-220. doi: 10.1002/2016SW001364.
- A. Bruno, et al. (2016). *Geomagnetically trapped, albedo and solar energetic particles: Trajectory analysis and flux reconstruction with PAMELA*. Adv. Space Res., doi:10.1016/j.asr.2016.06.042.
- A. Bruno, et al. (2016). *The May 17, 2012 solar event: back-tracing analysis and flux reconstruction with PAMELA*. J. Phys.: Conf. Ser. 675 032006.